Increasing Coverage and Maximum CFO in DFT-s-OFDM for Machine-Type Communications

Javier Lorca
Radio Access Networks Innovation
Telefónica I+D
Madrid, Spain
e-mail: franciscojavier.lorcahernando@telefonica.com

***Abstract*— One of the growing fields of interest in cellular communications is Machine-Type Communications (MTC). MTC traffic can be characterized in many applications by very low bit rates while requiring a high degree of coverage and reliability. Studies on how to increase coverage and reduce device costs have been extensively performed in DFT-s-OFDM due to its lower peak-to-average power ratio. Among the drawbacks of using DFT-s-OFDM for MTC are the Carrier Frequency Offset (CFO) requirements (thus precluding the use of low-cost local oscillators) and poor performance when coverage is limited (thus precluding devices with low transmission power). A common approach for coverage enhancements is to reduce the signal bandwidth in order to increase the power spectral density, but this does not alleviate the frequency offset requirements. This paper proposes an alternative transmission scheme that increases coverage and supports larger frequency offsets compared to classical bandwidth reduction schemes in DFT-s-OFDM. Link-level simulations demonstrate the superiority of the proposed technique in terms of coverage and resilience against large frequency offsets, and put into question the traditional approach of reducing bandwidth for coverage improvements in OFDM systems.**

Keywords*— *DFT-s-OFDM, OFDM, LTE, carrier frequency offset, machine-type communnications, frequency synchronization.

I. INTRODUCTION

Machine-Type Communication (MTC) refers to the type of traffic generated by (or directed to) a number of connected machines (such as remote sensors, vending machines, vehicles, and so on) in a given network. Studies on MTC wireless communications are mainly focused on the enhancements in coverage and capacity that are required for the support of large numbers of such devices in wide areas. MTC traffic for some applications can be characterized by very low bit rates (of the order of few hundreds of bps), high latencies (from seconds to minutes), and a possibly large number of almost inactive devices camped in a single cell.

Requirements for MTC have been addressed by 3GPP since Release 8 [1]. In order to turn LTE into a cost-effective solution for MTC, studies on how to improve the radio access network procedures for MTC are being extensively performed [2] [3]. 3GPP Release 12 foresees several mechanisms to extend coverage and reduce device costs, and additional studies are also being conducted in order to reduce layer-3 signaling overhead as well as increase battery savings [4].

Although downlink coverage can be enhanced through several techniques (such as the use of broadcast channels [5]), the limiting link in terms of coverage is the uplink because of the device's limited transmission power. In order to minimize uplink coverage issues, a modified flavor of Orthogonal Frequency Division Multiplexing (OFDM) can be employed, namely Discrete Fourier Transform–spread–Orthogonal Frequency Division Multiplexing (DFT-s-OFDM), also known as Single-Carrier Frequency Division Multiple Access (SC-FDMA). DFT-s-OFDM benefits from reduced peak-to-average power ratio (PAPR) and thus higher efficiency than OFDM which in turn prolongs battery life. However performance can be severely degraded when devices are in poor coverage conditions or present significant transmit power restrictions. At the same time, tight frequency synchronization is required as in OFDM thus precluding inexpensive local oscillators with carrier frequency offset values larger than half the subcarrier width. In addition, MTC devices should be low-cost, low-powered terminals with very limited processing capabilities.

One of the most common solutions to improve coverage is to reduce the transmission bandwidth (BW) so as to boost the power spectral density of the signal [2], but even in that case the support of eventually large CFOs remains an issue. Conversely, a reduction in the symbol length allows for larger CFO values but increases the signal bandwidth, therefore reducing the power spectral density and worsening the coverage.

This paper explores a simple method to modify physical transmissions in DFT-s-OFDM in such a way that both coverage and frequency offset robustness are increased, while preserving the single-carrier nature of the modulation. These enhancements come at the cost of reduced bit rates for a given allocated bandwidth, which is not a serious drawback in low-rate MTC applications for which reliability and cost are determinant. Performance is compared with that of a classical BW reduction approach, in terms of minimum SNR and maximum CFO for a given Block Error Rate (BLER).

The rest of the paper is organized as follows. Section II describes the proposed transmission mechanism. Section III describes the corresponding receiver structure. Section IV compares link-level simulation results with those obtained with a classical BW reduction scheme, and finally section V is devoted to conclusions.

Part of this work has been performed in the framework of the FP7 project ICT-317669 METIS, which is partly funded by the European Union. The authors would like to acknowledge the contributions of their colleagues in METIS, although the views expressed are those of the authors and do not necessarily represent the project.

II. PROPOSED TRANSMISSION MECHANISM

This paper proposes to reduce the number of useful complex symbols in a given bandwidth by a factor *L* prior to the DFT spreading operation, just completing the available space with *L* repetitions of *M* modulated symbols. The value *L* x *M* must be equal to the number of subcarriers granted for the user, and therefore *L* must be an integer submultiple of the number of subcarriers reserved for transmission.

Repetitions in the time domain are seen as a sampling operation in the frequency domain, which translates into an increase in the power spectral density of the subcarriers by a factor $10\times\log(L)$ in dB. This is equivalent to reducing the bandwidth by a factor *L*, but contrary to common belief, keeping a larger bandwidth is preferable in terms of minimum required SNR for a given BLER. At the same time, as will be shown in section IV, the proposed changes allow for an increase in the maximum supported frequency offset by a factor *gcd*(*L*, *N*) when compared to standard DFT-s-OFDM, where *gcd* stands for the greatest common divisor operation and *N* is the DFT-s-OFDM symbol length.

In what follows uplink operation will be assumed for convenience but the described techniques and results can identically be applied to downlink without any major change.

A. Detailed transmitter chain

Fig. 1 shows an overview of the complete DFT-s-OFDM transmission chain.

The result of the repetition and the subsequent *LxM*–point DFT is equivalent to an *M*-point DFT followed by a modified subcarrier mapping block. This is detailed in Fig. 2, where *M* complex information symbols are repeated *L* times so as to construct the information block to be mapped over each DFT-s-OFDM symbol. Standard techniques modulate a block of N_{sc}^{UL} complex symbols according to the allocated bandwidth, and this paper proposes to split it into *L* repetitions of *M* symbols where *L* can be any suitable submultiple of the total number of complex symbols and $L\times M = N_{sc}^{UL}$. The amount of information available in each DFT-s-OFDM symbol will thus be reduced by a factor *L* compared to the case without repetition, therefore reducing the bit rate for a given BW.

After the DFT the spectrum will comprise a lower number of subcarriers than in standard DFT-s-OFDM, with *M* non-null subcarriers at digital frequencies which are multiples of *L*, and *L*-1 zeroes between each pair of non-null subcarriers. It is apparent that the SNR of the non-null subcarriers will be increased by a factor $10\times\log(L)$ dB so that the total power of the uplink signal is preserved.

The proposed procedure can also be viewed as a reduction of the effective DFT-s-OFDM symbol length in the time domain without increasing the subcarrier width. This symbol length reduction will be exploited at the receiver for increased resilience against large frequency offsets, as will be explained in section III.

After appropriate mapping of subcarriers to the allocated frequency resources, a frequency shift of *L*/2 subcarriers is

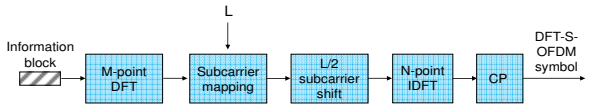

Fig. 1. Modified DFT-s-OFDM transmitter chain.

further applied in Fig. 1 for protection against both positive and negative frequency offsets. Subcarriers not used for transmission shall be set to zero up to the total number of subcarriers *N*. A subsequent *N*-length inverse DFT (IDFT) after appropriate padding with zeroes will deliver the time-domain DFT-s-OFDM symbols. Finally, insertion of the cyclic prefix completes the baseband DFT-s-OFDM symbol in the time domain.

The single carrier nature of DFT-s-OFDM is not compromised as the time-domain signal will comprise an up-sampled, frequency-shifted version of the original repeated complex symbols. Apart from the frequency shift (which is seen in the time domain as a complex weighting factor), the final uplink signal constitutes an up-sampled version of the original information containing *L* repetitions of the complex symbols, and transmission will be characterized by the same PAPR as in normal DFT-s-OFDM.

The null subcarriers in transmission will not be exploited for other users as happens in standard interleaved DFT-s-OFDM, where the spectrum occupied by each user is interleaved across the system bandwidth [6]. Instead, they will be explicitly blanked with the intention to aid the receiver in detecting signals with frequency offsets larger than half the subcarrier width, as will be shown in section III.

B. Relationship between the repetition factor and the DFT-s-OFDM symbol length

The *N*-point IDFT in Fig. 1 deserves further attention. Prior

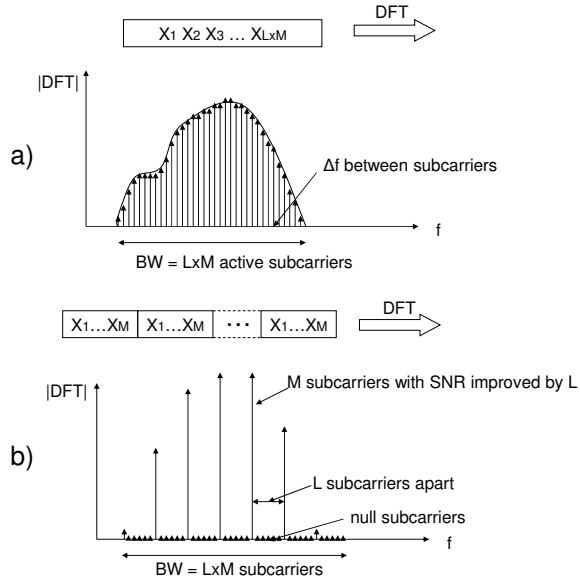

Fig. 2. Repetition of the complex symbols and resulting spectrum after the DFT: a) standard DFT-s-OFDM; b) proposal.

to the subcarrier mapping block, the spectrum in Fig. 2 has a sampling period of L subcarriers according to the repetition factor L. If N is a multiple of L, then after padding with zeroes the spectrum will show up the same sampling period in the frequency domain, and after the N-point IDFT the time-domain signal will comprise L repetitions. However, if N is not a multiple of L then the new sampling period L' will be given by $L' = \gcd(L, N)$. Choosing values of L that are also a submultiple of N ensures that the repetition pattern is maintained after the N-point IDFT, and this will be exploited by the receiver for increased robustness against large frequency offsets. If both L and N are primes then L' is equal to 1 and the signal will not comprise any repetitions in the time domain after the IDFT; it is therefore desirable that L' is as close as possible to L.

Fig. 3 shows the N-point spectrum in the case that L is not a submultiple of N. The spectrum can be viewed as being sampled with a period $L' = \gcd(L, N) < L$, and in the time domain this leads to repetition of L' blocks of samples. The figure shows the particular case of $L' = L/2$ for a better understanding. In this case the time-domain signal will comprise two repetitions of $N/2$ samples after the N-length IDFT in a given OFDM symbol.

III. Detailed Receiver Chain

In order to exploit the increased SNR of the transmit spectrum and the presence of null subcarriers the receiver will perform the processing steps illustrated in Fig. 4 and described in what follows.

- After CP removal, a frequency offset correction block will compensate the estimated CFO through multiplication of the samples in the time domain by the expression $\exp(-j2\pi\Delta\hat{f}_{off} n/N)$, where $\Delta\hat{f}_{off}$ is the estimated frequency offset, n is the index of the digital samples in the time domain, and N is the length of the OFDM symbol. The L' blocks of N/L' samples will offer increased protection against large frequency offsets between transmitter and receiver. Given that the frequency offset introduces a progressive phase factor of the form $\exp(j2\pi\Delta f_{off} n/N)$, where Δf_{off} is the actual frequency offset, CFO can be estimated as follows:

$$\Delta\hat{f}_{off} = -\frac{L'}{2\pi} Phase\left\{ \sum_{n=0}^{CP+N-N/L'-1} r[n] r^*[n + N/L'] \right\}. \quad (1)$$

In the above equation $r[n]$ represents the received samples in the time domain, CP is the length of the cyclic prefix and * denotes the conjugation operation. It is apparent that the sum is performed over most part of the received symbol, and frequency offset estimation can be greatly improved compared to standard techniques where the sum can only be applied over the cyclic prefix length [7].

The resolvable phases must be in the interval [-π, π] and this results in a maximum supported frequency offset given by $\Delta f_{off,\max} = \pm L' \times \Delta f / 2$. The maximum frequency offset is thus multiplied by a factor L' compared to standard DFT-s-OFDM.

- The frequency components of the received OFDM symbol are then shifted to baseband through multiplication of the samples in the time domain by a factor $w[n] = \exp(-j2\pi(\Delta + L/2)n/N)$. Here Δ represents the difference between the center of uplink resources and the DC subcarrier (measured in number of subcarriers).
- An N-point DFT is then performed in order to obtain the frequency components of the signal, followed by a channel equalization block that compensates channel impairments according to any suitable technique such as e.g. MMSE, Zero-Forcing or Maximum Likelihood.
- Finally, an M-point IDFT is further applied in order to de-spread the complex information symbols. The sampled spectrum before the IDFT can be exploited by restricting the IDFT only to the non-null subcarriers, thus removing part of the additive noise and reinforcing detection by a factor $10 \times \log(L)$ dB.

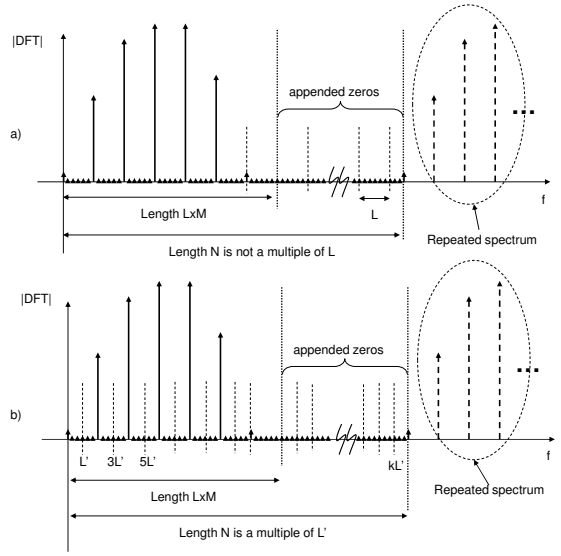

Fig. 3. N-point spectrum when L is not a submultiple of N, for the particular case L'=L/2: a) sampled with period L; b) sampled with period L'.

L shall preferably be an integer submultiple of N so that $L' = L$ and the supported frequency offset is maximized. L shall also be a submultiple of the number of allocated subcarriers. As the power spectral density will be improved by a factor $10 \times \log(L)$ dB regardless of the value of L', L should be the maximum integer that fulfils the condition of being a submultiple of both N and N_{sc}^{UL}. Selection of L should be made by the base station according to the actual CFO between the transmitter and receiver, which is clearly dominated by the device's characteristics. To this end, the device could send a

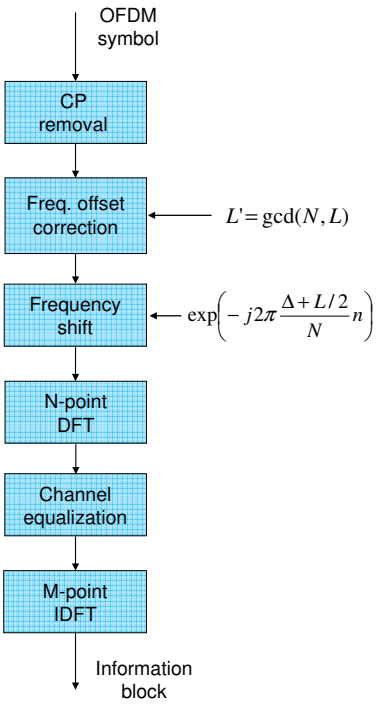

Fig. 4. Modified DFT-s-OFDM receiver chain

rough estimation of its maximum CFO to the base station so that the optimum value of L can be chosen and appropriately signaled to the device.

In addition, both the amount of information to be sent and the value L determine the bandwidth to be allocated. This bandwidth should be higher than the channel coherence bandwidth in order to maximize the frequency diversity and thus improve detection. The base station should therefore employ values of L that lead to user bandwidths greater than the channel coherence bandwidth, which is assumed to be known by the base station by means of measurements or direct reporting from the devices.

IV. Simulation Results

In order to analyze the benefits of the proposed technique, a number of link-level simulations were performed for the uplink of LTE in different configurations. The simulation assumptions are collected in Table I. Four values of the repetition factor L were analyzed (2, 4, 6 and 8), as well as the no repetition (L = 1) case. The channels considered were ITU Extended Pedestrian A (EPA) and ITU Extended Vehicular A (EVA) with 3 km/h and no shadowing. The selected modulation and coding scheme was QPSK 1/5. The applied CFO was changed from 0 to two times the subcarrier width (Δf = 15 kHz), and BLER statistics were collected under a standard LMMSE equalizer with 1 RX antenna. Channel estimation was ideal in order to isolate its impact from the proposed scheme. CFO estimation was realistic, precluding any averaging technique.

User bandwidths were chosen according to the 50% coherence bandwidth as given by the expression $B_{c,50\%} = 1/(5\sigma_\tau)$, where σ_τ is the r.m.s. delay spread [3]. This expression yields the values collected in Table II. The selected user bandwidths for L = 1 were 10 RB and 2 RB respectively for each channel type (corresponding to 552 kbps and 91 kbps, respectively), lower than the channel coherence bandwidths. L = 1 thus resembles the classical BW reduction approach, and user bandwidth is multiplied by L when applying the proposed L-spreading technique with L > 1. Performance could thus be compared for the same bit rate and different values of L.

Figs. 5 and 6 show BLER vs. SNR curves obtained for the EPA and EVA cases respectively with CFO = 0. It is apparent that increased values of L result in a lower SNR for a given BLER, and the proposed technique outperforms the classical BW reduction approach thanks to the extra frequency diversity that is re-gained by the L-spreading operation. Figs. 7 to 14 show analogous curves for CFO = 0.25Δf, 0.5Δf, Δf and 2Δf in EPA and EVA channels. It is apparent that higher values of L enable detection at lower SNR and higher CFO, with an optimum value given by L = 6 for moderate CFO values (lower than Δf). L = 4 and L = 8 are the only possibilities for CFO = Δf, and L = 8 allows for coping with the case CFO = 2Δf. The behavior of L = 8 with non-zero CFO will be analyzed later.

The described results can be better condensed in Table III.

TABLE I. Simulation Assumptions

Parameter	Setting
Carrier frequency	2.6 GHz
System bandwidth	20 MHz (100 RBs)
User bandwidth	See Table II
Modulation and Coding Scheme	QPSK 1/5
Subcarrier spacing (Δf)	15 kHz
Channel types	ITU EPA and EVA, 3 km/h, no shadow fading
Channel estimation	Ideal
CFO estimation	Realistic, no averaging of CFO values over multiple subframes
Receiver scheme	LMMSE, 1RX
Turbo decoder iterations	8
No. erroneous blocks	800
Repetition factor L	1, 2, 4, 6, 8
Carrier Frequency Offset	0, 0.25Δf, 0.5Δf, Δf, 2Δf

TABLE II. 50% Channel Coherence Bandwidth, and Allocated User Bandwidth for the Simulations

Channel type	50% channel coherence bandwidth (kHz)	50% channel coherence bandwidth (RB)	User BW (RB)
EPA	4651.1	25.8	10L
EVA	560	3.1	2L

TABLE III. REQUIRED SNR VALUES FOR 1% BLER

CFO	Case	*L*=1	*L*=2	*L*=4	*L*=6	*L*=8
0	EPA, 552 kbps	4	1.5	-0.8	-2	-3.3
	EVA, 91 kbps	-4.7	-7	-9.2	-10	-10.5
0.25Δ*f*	EPA, 552 kbps	20	14	12.8	10.8	13.5
	EVA, 91 kbps	∞	2.5	2.5	1	4.5
0.5Δ*f*	EPA, 552 kbps	∞	14	13	10.7	13.5
	EVA, 91 kbps	∞	2.1	2.5	1	4.5
Δ*f*	EPA, 552 kbps	∞	∞	13	∞	13
	EVA, 91 kbps	∞	∞	2.5	∞	4.5
2Δ*f*	EPA, 552 kbps	∞	∞	∞	∞	13.5
	EVA, 91 kbps	∞	∞	∞	∞	4.5

This table collects the SNR values (in dB) required at 1% BLER for L = 1, 2, 4, 6 and 8 and different values of the CFO and channel model. It is apparent that the SNR values greatly decrease with L, with some saturation observed beyond L = 6 for CFO = 0, and an unexpected increase with L = 8 for CFO = 0.25Δf and CFO = 0.5Δf. L = 6 thus presents the best performance for CFO values up to 0.5Δf. For CFO = Δf a value L = 4 is the best option because L = 8 does not yield any improvements (L = 6 is not an option in this case as it supports the same maximum CFO as L = 2). The largest CFO (2Δf) can only be supported with L = 8.

The required SNR for L = 8 is higher than expected with non-zero values of the CFO. This is due to the DFT operation that spreads the effects of channel impairments over all the allocated subcarriers, thus degrading performance when the user bandwidth is much larger than the channel coherence bandwidth (especially in EVA). Good choices for both channel models are thus L = 6 when CFO is not higher than 0.5Δf; L = 4 when CFO = Δf; and L = 8 when CFO = 2Δf. CFO values beyond 2Δf would require correspondingly higher values of L.

The base station should take into account the maximum reported CFO and the channel coherence bandwidth for appropriate selection of L. This selection could be performed upon initial establishment of the connection between the MTC device and the network, in which the device could also report a list of supported values of L according to its capabilities.

V. CONCLUSIONS

This paper describes a simple yet effective way to increase coverage and robustness against large carrier frequency offsets in DFT-s-OFDM, by introducing repetitions of the complex symbols prior to the DFT operation and exploiting the increased subcarrier separation at the receiver. The proposed mechanism improves the required SNR for a given BLER compared to traditional strategies based on simple reduction of the user bandwidth, because the extra frequency diversity helps in the detection at the cost of increased user bandwidth. Additionally, CFO values larger than half the subcarrier width

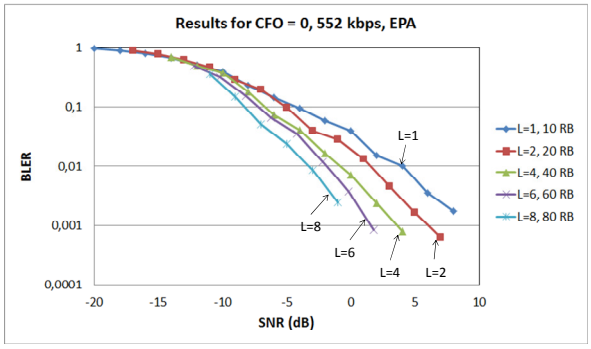

Fig. 5. Simulation results, EPA channel model, 552 kbps, CFO = 0.

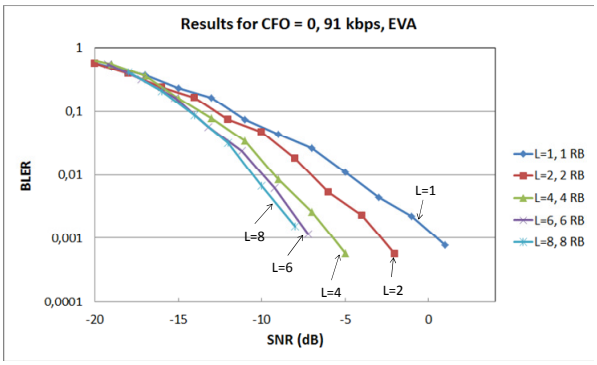

Fig. 6. Simulation results, EVA channel model, 91 kbps, CFO = 0.

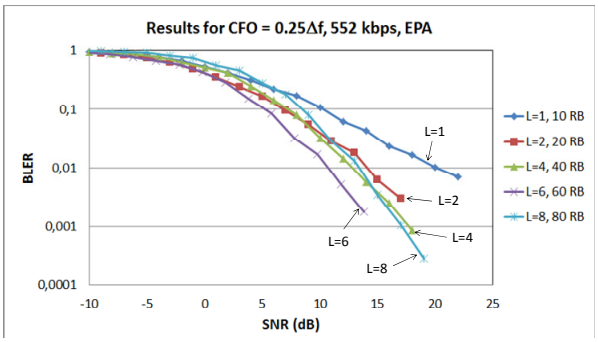

Fig. 7. Simulation results, EPA channel model, 552 kbps, CFO = 0.25Δf.

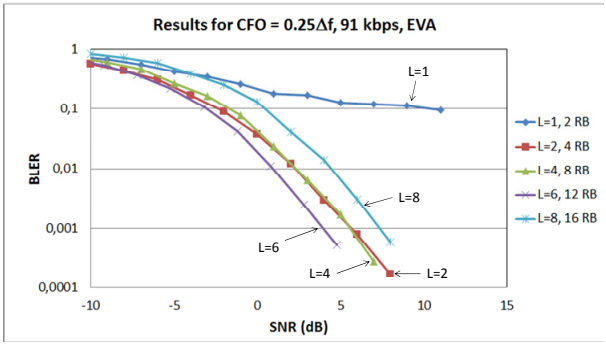

Fig. 8. Simulation results, EVA channel model, 91 kbps, CFO = 0.25Δf.

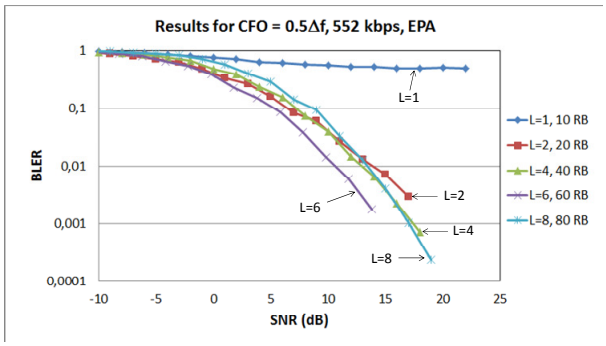

Fig. 9. Simulation results, EPA channel model, 552 kbps, CFO = 0.5Δf.

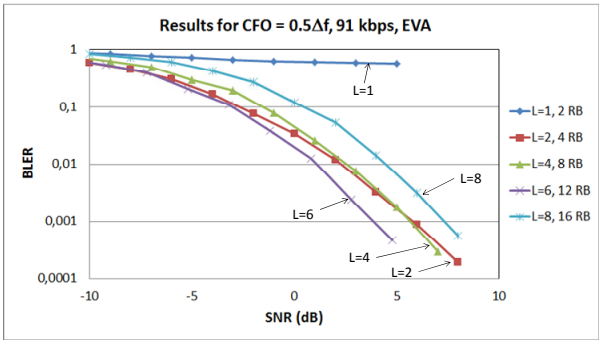

Fig. 10. Simulation results, EVA channel model, 91 kbps, CFO = 0.5Δf.

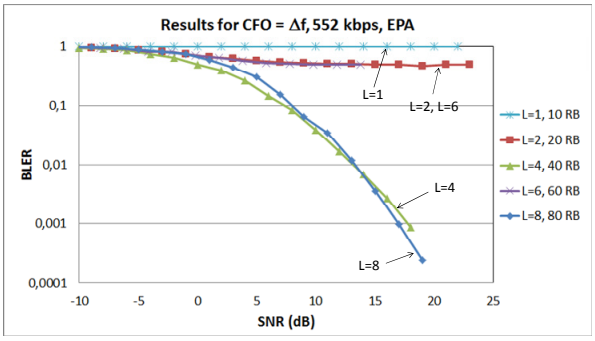

Fig. 11. Simulation results, EPA channel model, 552 kbps, CFO = Δf.

can be supported by using appropriate values of the repetition factor *L*, thanks to the extra separation between subcarriers. Both characteristics aid in the deployment of low-cost MTC devices with poor coverage and/or frequency stability characteristics. Simulations show very good results with values of *L* between 2 and 8 leading to significant improvements in both coverage and maximum supported CFO. Future investigations will be conducted in order to extend this approach to reference signals for enhanced channel estimation.

REFERENCES

[1] 3GPP TR 22.868 (March 2007), "Facilitating Machine to Machine Communication in 3GPP Systems".

[2] J. Berglund, "Extended LTE Coverage for Indoor Machine Type Communication", Dept. Elect. Engin., Linköping Univ., June 2013.

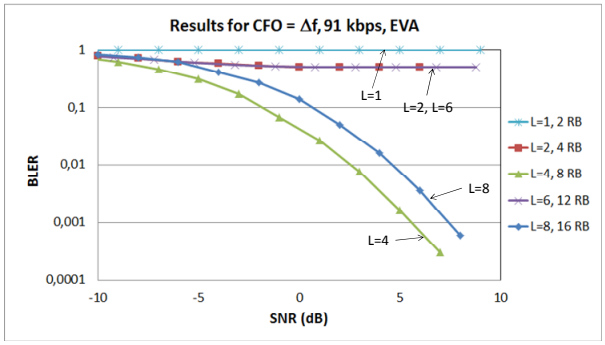

Fig. 12. Simulation results, EVA channel model, 91 kbps, CFO = Δf.

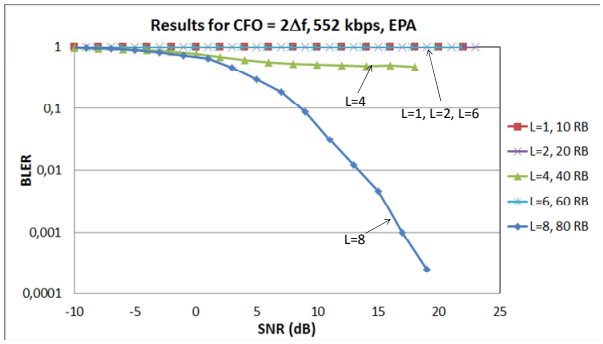

Fig. 13. Simulation results, EPA channel model, 552 kbps, CFO = 2Δf.

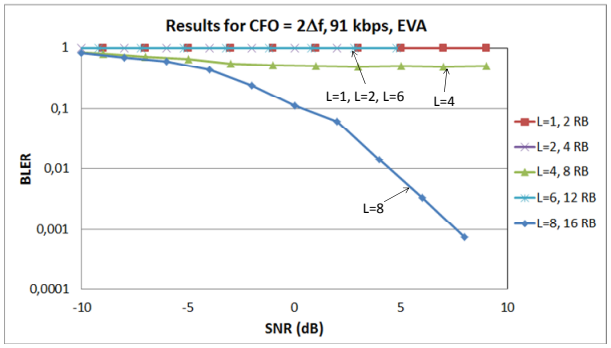

Fig. 14. Simulation results, EVA channel model, 91 kbps, CFO = 2Δf.

[3] S. Andreev, A. Larmo, M. Gerasimenko, V. Petrov, O. Galinina, T. Tirronen, J. Torsner, and Y. Koucheryavy, "Efficient Small Data Access for Machine-Type Communications in LTE", IEEE International Conference on Communications (ICC), 2013.

[4] 3GPP TR 37.869 v0.2.0 (April 2013), "Study on Enhancements to Machine-Type Communications (MTC) and other Mobile Data Applications; Radio Access Network (RAN) aspects".

[5] S. Shieh, Y. Chen, "Channel Decoder Design of Physical Broadcast Channel for Coverage Enhancement in LTE", Int. J. of Science and Engineering, vol. 4 (1), pp. 365-367, 2014.

[6] S. Sesia, I. Toufik, M. Baker (eds.), LTE – the UMTS Long Term Evolution: From Theory to Practice, 2nd ed. United Kingdom: Wiley, 2011.

[7] J.J. van de Beek, M. Sandell, and P.O. Börjesson, "ML Estimation of Time and Frequency Offset in OFDM Systems", IEEE Trans. Signal Proc., vol. 45 (7), pp. 1800–1805, July 1997.